



저작자표시-비영리-변경금지 2.0 대한민국

이용자는 아래의 조건을 따르는 경우에 한하여 자유롭게

- 이 저작물을 복제, 배포, 전송, 전시, 공연 및 방송할 수 있습니다.

다음과 같은 조건을 따라야 합니다:



저작자표시. 귀하는 원저작자를 표시하여야 합니다.



비영리. 귀하는 이 저작물을 영리 목적으로 이용할 수 없습니다.



변경금지. 귀하는 이 저작물을 개작, 변형 또는 가공할 수 없습니다.

- 귀하는, 이 저작물의 재이용이나 배포의 경우, 이 저작물에 적용된 이용허락조건을 명확하게 나타내어야 합니다.
- 저작권자로부터 별도의 허가를 받으면 이러한 조건들은 적용되지 않습니다.

저작권법에 따른 이용자의 권리는 위의 내용에 의하여 영향을 받지 않습니다.

이것은 [이용허락규약\(Legal Code\)](#)을 이해하기 쉽게 요약한 것입니다.

[Disclaimer](#)

공학석사 학위논문

Self Ignition Phenomena of High Pressure Hydrogen Released into Tube with Diaphragm Rupture Conditions

튜브 내 누출되는 고압수소의
격막파열조건에 따른 자발점화 현상

2015년 2월

서울대학교 대학원
기계항공공학부
임 한 석

Abstract

Self Ignition Phenomena of High Pressure Hydrogen Released into Tube with Diaphragm Rupture Conditions

HanSeuk Lim

School of Mechanical and Aerospace Engineering
The Graduate School
Seoul National University

High combustion efficiency of hydrogen could make it an ideal source of green energy in the future. At this time, high pressure vessel is the most reasonable method of storing hydrogen. However, such a high pressurized vessel could pose a critical threat if ruptured. For this reason, it is important to understand the mechanism of hydrogen's self-ignition when a high-pressure hydrogen is released into air. This paper presents several visualization images as experimental results using a high-speed camera. From the visualization images, the ignition is initiated near the rupture disk immediately after failure of the disk. And the early ignition and flame is stronger as a rupture pressure increases. However, this ignition region does not affect the general self-ignition mechanism when high-pressure hydrogen is released into the air through tube after failure of disk.

Key Words: High-pressure hydrogen, Self-ignition, Hydrogen-air Mixing, Flow visualization

Student Number : 2013-20708

Contents

Abstract	i
Contents	ii
List of Tables	iii
List of Figures	iv
Chapter 1 Introduction	1
1.1 Background	1
Chapter 2. Literature Review	3
2.1 Characteristics of hydrogen	3
2.2 Previous study on high pressure hydrogen self ignition	4
Chapter 3. Experimental Setup	5
3.1 Test model	5
3.2 Visualization and pressure measurement	9
3.2.1 Visualization	9
3.2.2 Pressure transducers	11
3.3 Safety chamber	13
3.4 Test procedure	13
Chapter 4. Results and Discussion	15
4.1 Test results summary	15
4.2 Test results	19
4.2.1 Low pressure test	21
4.2.2 High pressure test	24
Chapter 5. Conclusion	31
Bibliography	32
초 록	34

List of Tables

Table 1	Frequency of occurrence of ignition sources [1]	2
Table 2	Comparative properties of hydrogen and fuels	3
Table 3	Specifications of Phantom V710/V2511	10
Table 4	Test conditions	15
Table 5	Summery of test; theoretical shock speed.	19

List of Figures

Figure 1 Test configuration and safety chamber	6
Figure 2 Test configuraton schematic	6
Figure 3 Test model draft	7
Figure 4 Test model	7
Figure 5 Test Mylar film (Left : after rupture, Right : before rupture)	8
Figure 6 Optical access window.	8
Figure 7 Phantom V710	10
Figure 8 Phantom V2511	10
Figure 9 PCB pressure transducer 111A26	12
Figure 10 Kulite ETM-HT-375	12
Figure 11 Sensys PMHA 1000	12
Figure 12 Shadow image of hydrogen experiment and helium experiment.	16
Figure 13 Representative test result (Test #90)	17
Figure 14 Leading shock wave and mixing zone model schematic [12]	20
Figure 15 Wall static pressure of extension tube; Test #77	22
Figure 16 Shadowgraph image, entire area, non-ignition; Test #77	22
Figure 17 Wall static pressure of extension tube; Test #81	23
Figure 18 Shadowgraph image, entire area, non-ignition; Test #81	23
Figure 19 Wall static pressure of extension tube; Test #89	25
Figure 20 Wall static pressure of extension tube; Test #90	26
Figure 21 Wall static pressure of extension tube; Test #91	26
Figure 22 Upstream area visualization of test #89	27
Figure 23 Upstream area visualization of test #90	28
Figure 24 Upstream area visualization of test #91	29
Figure 25 Wall static pressure of extension tube; Test #92	30
Figure 26 Upstream area visualization of test #92	30

Chapter 1 Introduction

1.1 Background

In the 21st century, the concern about global warming and atmospheric pollution made demand for clean carbon-free fuel high[1]. after Kyoto Protocol take effect, many advanced countries are under develop to alternated energy source then fossil fuel. the Hydrogen has been expected as future energy source or fuel because of high combustion efficiency and high energy per unit mass. in addition, hydrogen produces only H_2O water vapor when it burn. this feature makes hydrogen as clean green carbon-free energy.

one of the most researched field for commercial usage of hydrogen fuel is automobile. Many major automobile companies tried to develop and commercialize the hydrogen car. by hydrogen fuel cell or hydrogen inertial combustion engine.

For hydrogen fuel application, enough amount of hydrogen should stored. hydrogen has low energy content density that makes it hard to store. there were three method for storing hydrogen. compressed gas vessel, liquefied vessel, and a hydrogen storing alloy. But hydrogen storing alloy is technically limited. so two methods are the only possible method. Liquefied storing is mostly used in space launch vehicle. but liquefied hydrogen is hard to handling, to store long term, and to apply to common use because necessity of re-vaporizer. In these reasons, compressed gas vessel is the most probable method for commercial hydrogen storing even if it has several disadvantages.

Safety issue is one of the most considerable disadvantage of compressed

gas vessel methods. Every flammable gas has potential hazards about accidental fire or explosion especially when they are highly compressed. In the past, it is believed that even high compressed flammable gas, if it is isolated from any ignition source, there were no chances of fire or explosions. But many hydrogen accident show that they occur even if there were no identified ignition source. According to the Major Hazard Incident Database Service (MHIDAS), only 11cases of total 81 hydrogen involved incidents are ignition source identified.

Table 1 Frequency of occurrence of ignition sources [1]

Ignition source	Hydrogen incidents		Non-hydrogen incidents	
	Number	%	Number	%
Arson	0	0	37	2.6
Collision	2	2.5	121	8.4
Flame	3	3.7	113	7.9
Hot surface	2	2.5	56	3.9
Electric	2	2.5	114	7.9
Friction spark	2	2.5	33	2.3
Not identified	70	86.3	942	65.5
Non-ignition	0	0	21	1.5
Total	81	100.0	1437	100

For these un-identified ignition incidents, many postulated mechanisms were introduced. First, the reverse Joule-Thomson effect was postulated. several electrostatic ignitions mechanisms are also postulated include spark discharged from conductors, brush discharges, and corona discharges. Sudden adiabatic compression mechanism and a hot surface ignition mechanism also postulated. In this time, the most probable postulated mechanism for released hydrogen self-ignition, is the diffusion ignition introduced by Wolanski and Wojcicki[2]. They used a shock tube, to demonstrate that high pressure hydrogen released into air or oxygen, it could be ignited while they are expanding. In this thesis, we see more details in diffusion ignition mechanism and self-ignition visualization Then previous studies.

Chapter 2. Literature Review

2.1 Characteristics of hydrogen

Hydrogen is promising future energy source. Hydrogen is the lightest material in the world, also it has the highest combustion energy per unit mass material in the world. Comparative Properties of hydrogen and fuels are shown as Table. 2.

Table 2 Comparative properties of hydrogen and fuels

Properties	Hydrogen	Methan	Propane	Methanol	Ehanol	Gasoline	Notes/ Sources
Chemical Formula	H ₂	CH ₄	C ₃ H ₈	CH ₃ OH	C ₂ H ₅ OH	C _x H _y (x=4-12)	
Molecular Weight	2.02	16.04	44.1	32.04	46.07	100-105	[a,b]
Density (NTP) kg/m ³	0.0838	0.668	1.87	791	789	751	[a,c]
Viscosity (NTP) g/cm-sec	8.81x10 ⁻⁵	1.10x10 ⁻⁴	8.012x10 ⁻⁵	9.18x10 ⁻³	0.0119	0.0037 - 0.0044	[a,b]
Normal Boiling Point °C	-253	-162	-42.1	64.5	78.5	27 - 225	[a,b]
Flash Point °C	< -253	-188	-104	11	13	-43	[b,d]
Flammability in Air vol%	4.0 - 75.0	5.0 - 15.0	2.1 - 10.1	6.7 - 36.0	4.3 - 19	1.4 - 7.6	[a,b]
Auto-Ignition Temp. in Air °C	585	540	490	385	423	230 - 480	[b,d]

Sources:

[a] : NIST Chemistry WebBook. <http://webbook.nist.gov/chemistry>

[b] : "Alternatives to Traditional Transportation Fuels: An Overview." DOE/EIA-0585/0. Energy Information Administration. U.S. Department of Energy. Washington, DC. June 1994

[c] : Perry's Chemical Engineers' Handbook (7th Edition), 1997, McGraw-Hill

[d] : Hydrogen Fuel Cell Engines and Related Technologies. Module 1: Hydrogen Properties." U.S. DOE. 2001, http://www.eere.energy.gov/hydrogenandfuelcells/tech_validation/pdfs/fcm01r0.pdf

2.2 Previous study on high pressure hydrogen self-ignition

There were several studies on the diffusion ignition which postulated for mechanism of the self-ignition of high pressure hydrogen suddenly released into tubes[3-12]. Studies on self-ignition explained by diffusion ignition are performed by Dryer et al. [3], Mogi et al.[4-5], Golub et al. [6-8], Lee and Jeung [10], and Wen et al [11]. Dryer et al. [3] suggested that multi-dimensional shock interaction induced by the disk bursting may influence mixing of hydrogen and air, which can generate the self-ignition. Dryer et al. [3] experiment hydrogen self-ignition with various metal rupture disks, and various length extension tubes. They found out self-ignition are influenced by burst pressure and tube length. Figure 1.

An experimental study of Mogi et al. [4-5] with various extension tube length and inner diameter shows that the burst pressure of the diaphragm and the tube length had a relationship with the self-ignition of high pressure hydrogen release through the tube.

Golub et al. conducted a comparative study with a circular and rectangular cross section tube. they found that burst pressure for self-ignition was lower with a rectangular cross section tube than the circular section tube. They explained that the mixing process is enhanced in rectangular cross section by three dimensional effects.

Chapter 3. Experimental Setup

3.1 Test model

For experimental research, an extension tube model was made. The model consist of a storage cylinder, diaphragm and an extension tube with visualization window. model was made with aluminium. the storage cylinder's inner diameter is 25mm and 190mm long. the cylinder wall has flange to connect the extension tube part. one side of cylinder is fully open and surrounded by an O-ring. When the test model is assembled this side is closed by diaphragm. O-ring and Mylar diaphragm seals the cylinder.

The extension tube consists of 6 parts. The upper and lower plate, two visualization windows and two holding arms. For inner flow visualization, the extension tube inner cross section was made in a square shape. When the test was conducted, the extension tube got high stresses, so it should be thick enough to stand it.

The visualization windows are 15mm thick pyrex glasses. Pyrex glass has higher transmittance and structural and thermal strength than normal glasses. Because of test required high visibility and test environment are extreme, Pyrex glass was used for the visualization window.

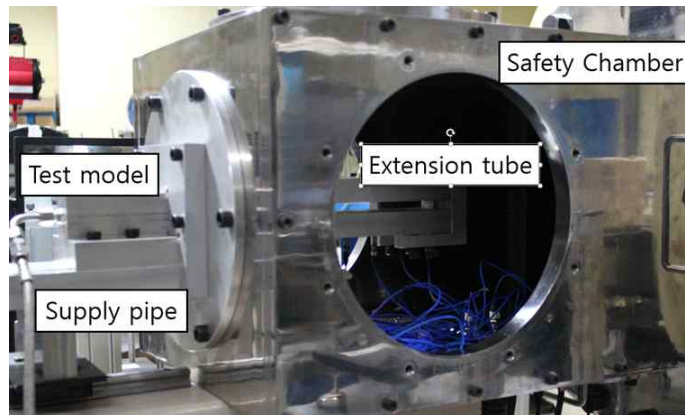


Figure 1 Test configuration and safety chamber

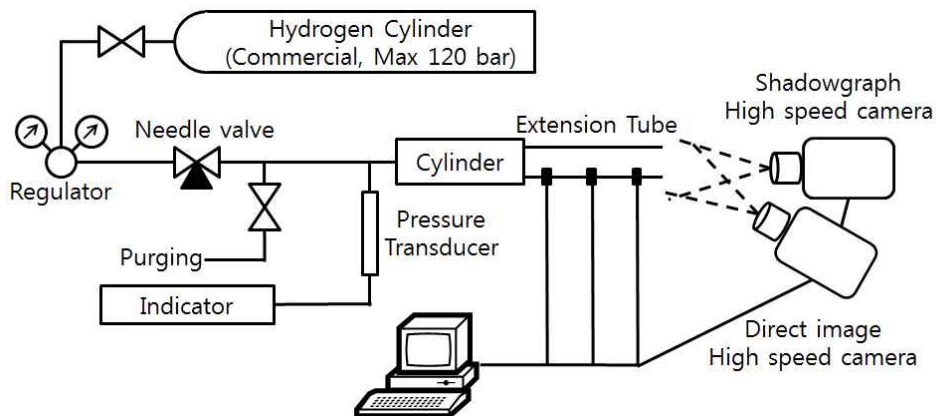


Figure 2 Test configuration schematic

The upper and lower part is made by aluminium. The upper and lower plate has two grooves for visualization window. During test flow moving through extension tube, the shock could brake the visualization window. To prevent this, paper or rubber gaskets are installed between grooves and windows. The window groove shape is trapezoid to prevent the window moving longitudinal direction. The lower part has 6 ports for pressure transducers. pressure transducers are used to measure shock speed and

strength. The first port is 21mm away from the diaphragm, and after the first port, ports are located in every 34.8mm.

The extension tube parts are assembled with to cylinder flange. Each part has 6 holes. There is a total of 12 bolts holding the tube parts to the cylinder. The tube is made of 4 parts. To maintain the tube cross section as parallel, two holding arms are installed. The upper and lower plate have 4 ports for holding arms at the outside of the tube exit.

extension tube has 10mm width, 10mm height square cross section and 200mm length.

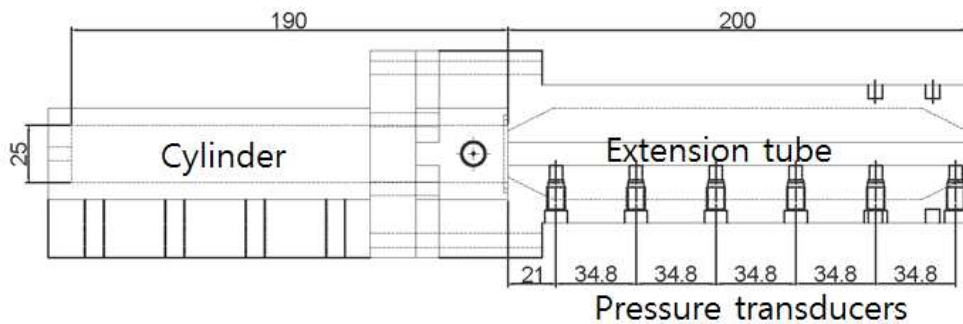


Figure 3 Test model draft

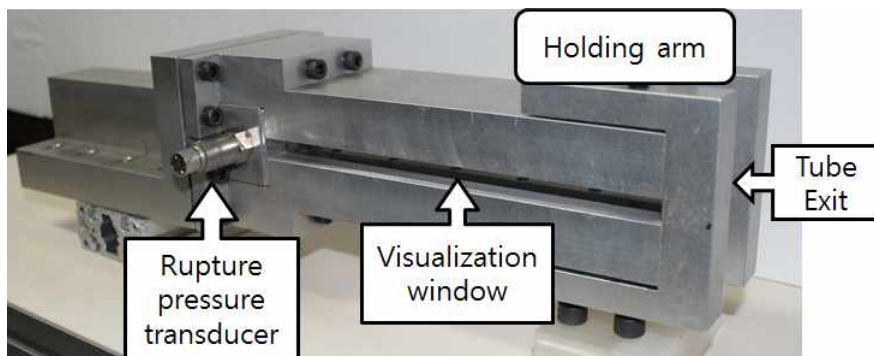


Figure 4 Test model

Mylar(Polyethylene terephthalate, PET) films are used for the diaphragm. By using variant thick film, we control rupture pressure. there are $25\text{ }\mu\text{m}$, $50\text{ }\mu\text{m}$, $100\text{ }\mu\text{m}$ thick film used.

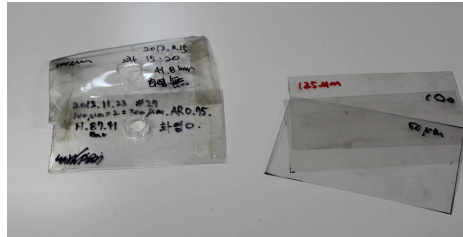


Figure 5 Test Mylar film (Left : after rupture, Right : before rupture)



Figure 6 Optical access window.

3.2 Visualization and pressure measurement

3.2.1 Visualization

For Visualization, Z-type Focused shadowgraph method with high speed camera was applied. Also a direct image also taken by high speed camera. Direct images are used for observing the reaction area or frame itself. Videos from shadowgraph and direct image are synchronized by signal from the first pressure transducer. In this study, two high speed cameras were used. due to specifical differences between the two cameras, camera settings are limited and traded off. The shadowgraph camera set twice frame per second then the direct camera to synchronization of two videos. shadowgraph images applied as two area. First, entire tube areas(200mm) are observed. Second, for observe formation of leading shock and phenomena in rupture moment in detail, the 80mm of upstream are observed. Interval between frames are $1.8 \mu s$ for upstream shodow graph images, $2.8 \mu s$ for entire tube area shodow graph images and $5.5 \mu s$ for direct image. A Xenon lamp is used as the light source the shadow graph images. For definite image, exposure time should be minimum. but exposure times are limited by light source brightness. The shadow graph image exposure time is limited as $0.5 \mu s$ and direct image exposure time limited to $1 \mu s$.

The phantom V2511 and V710 high speed cameras are used for this experiment. This study is more focused on the shadowgraph and V2511's performances are about double then V710. so V2511 used for shadowgraph and V710 used for direct image. the specifications of cameras are as follows.



Figure 7 Phantom V710



Figure 8 Phantom V2511

Table 3 Specifications of Phantom V710/V2511

	V710	V2511
Maximum capacity (optional)	1,400,000 pictures-per-second	1,000,000 pictures-per-second
Resolution	128x8(min) to 1280x800(max)	128x16(min) to 1280x800(max)
Imaging sensor	CMOS sensor 1280 x 800 pixels	CMOS sensor 1280 x 800 pixels
Pixel size	20 μ m	28 μ m

3.2.2 Pressure transducers

For measuring rupture pressure and shock strength, some pressure transducers are applied to the test model. In this study, three kinds of pressure transducers are used. Kulite ETM-HT-375 series, Sensys PMHA 1000 series and PCB Piezotronics 111A26 series. Kulite and Sensys pressure transducers are used for measuring burst pressure. For measuring burst pressure, a pressure transducer is installed just upstream of the diaphragm. But near the diaphragm area, there is a potential risk that when the diaphragm is ruptured and self-ignition can occur, and high temperature from the ignited flame could cause damage to the pressure transducer. Kulite ETM-HT-375 is a pressure transducer that has a high temperature resistance when using it in a high temperature condition or extreme environment. Also a common commercial pressure transducer, Sensys PMHA 1000 is applied to the supply valve. These two sensors are used to measure rupture condition. The only way to measure rupture pressure is by using a pressure transducer, so in this study, we use two pressures to ensure the measured values are reasonable. The differences between two transducers are very small. Especially, when the hydrogen cylinder inner pressure goes over 20 bar, the difference is only under 0.3 bar.

As mentioned previously, the extension tube under plate has 6 ports for PCB Piezotronics pressure transducers. The 111A26 model was chosen by expected experimental conditions from a shock tube theory. Because shocks and self-ignition flames are very fast and have a short time phenomena, piezoelectric type transducers are only applicable in the shock tube.



Figure 9 PCB pressure transducer 111A26



Figure 10 Kulite ETM-HT-375



Figure 11 Sensys PMHA 1000

3.3 Safety chamber.

The experiment was conducted in a safety chamber to avoid fire safety problems and noise issues. The safety chamber consists of a test section, a dump tank, and an optical access window. the test section is made from a 20mm thick stainless steel plate. It has a 300mm inner width, 300mm inner height and 600mm inner length. Test section consist removable side plate, upper and lower plate, and the test model adaptor. the lower plate has a multiple BNC connector. All the pressure transducer signals from the test model to data acquisition board are connected through this connector.

The model adapter holds the test model in the test section. Hydrogen gas is supplied to here.

The cylindrical dump tank has about 2 m³ volume. The dump tank and test section has a large volume relative with test model, and closed space effects are expected to be small enough to ignore.

3.4 Test procedure

The experimental was study conducted with the following sequences. First for the experimental setup sequence, we assembled the test model with selected specific thickness of diaphragm. The test model installed in the safety chamber test section. In this sequence, all pressure transducers were connected to DAQ via BNC cable. The hydrogen supply pipe was also connected to cylinder via Swagelok. All the sensors, transducers, cameras triggers are synchronized with a signal of the first pressure transducer in the extension tube. All the cable connection and trigger were checked before closing the test section. The model install and data cable and pipes are all

connected. then assembled safety chamber side plate and optical access window.

After the experimental setup sequence, then test sequence is started. The hydrogen supply pipe has a needle valve. With this valve, control hydrogen feeding mass flow according rupture pressure transducer to feed is not so fast. If feeding speed is too fast, diaphragms are bursted at a lower and irregular cylinder pressure. Also the feeding speed is fast, the difference of two rupture pressure transducer values goes larger. This is because that feeding speed is fast mean hydrogen flow that going into the cylinder has high speed and get a dynamic pressure. For regular rupture feeding speed must be controled. In this study, we control feeding speed by two rupture pressure transducers difference remain in 1bar. If feeding speeds are controled properly, rupture pressures are almost regular according to diaphragm thickness. In the same diaphragm thickness rupture pressures are in ± 3 bar. Diaphragm ruptures, leading shock was developed and pressure behind of shock goes high. When leading shock reaches the first pressure transducer, the trigger activated all the pressure transducers and cameras. Because there were gaps in the diaphragm and first pressure transducer, every transducer and camera should use a pre-trigger. In our experiment condition, entire process completed in $300\mu s$. time gap between diaphragm rupture and pressure transducer trigger is less then $150\mu s$. so our high speed camera and pressure transducers set pre-trigger as $200\mu s$. acquired data are arranged and saved in DAQ computer. After diaphragm rupture, check the self-ignition flame of extension tube exit. and close hydrogen supply valve. The close supply valve, and the fire in the extension tube exit extinguished (if it occurs), then disassemble test section side plate, detach pressure transducer and hydrogen supply pipe, and disassemble test model. and the test sequence and the experiment are finish.

Chapter 4. Results and Discussion

4.1 Test results summary

High pressurized hydrogen has released into tube by diaphragm rupture. Flow and shock development captured by shadowgraph image. [table] shows test conditions and results. Rupture pressure is controled by film thickness. Self-ignition takes place when rupture pressure is over 80 bar. Test conditions are limited, so we could not find a failed ignition condition. Under 50 bar, it is always non ignition. and over 80 bar, it is self-ignition always.

Table 4 Test conditions

Test #	Test gas	Rupture pressure (MPa)	Diaphragm thickness (μ m)	Self-ignition	Early flame
#77	Helium	4.1	100	No	no
#81	Hydrogen	4.3	100	No	no
#89	Hydrogen	8.6	200	Yes	yes
#90	Hydrogen	8.6	200	Yes	yes
#91	Hydrogen	9.2	219	Yes	yes
#92	Hydrogen	9.4	219	Yes	no

Figure 12 shows that non-reaction shadowgraph image result using test gas as helium. this is for observing flow development without reactions. Generally, there were no large differences between test result and former numerical researches but the shock propagate speed are different because of molecular weight differences between hydrogen and helium.

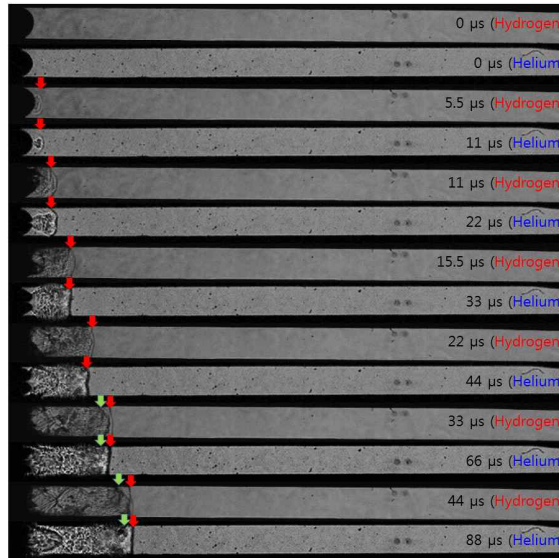


Figure 12 Shadow image of hydrogen experiment and helium experiment.

Figure 13 shows the representative shadowgraph and direct image result from tests. General flow development is like this. first, just after rupture. from a small rupture hole in the diaphragm, small shocks are occurring and propagating into the entire tube cross section. Because the diaphragm hole is also enlarged so propagating shock is distorted bow shock shape. Because of bow shocks development, reflection from tube wall, and flow distortion from diaphragm edges, the flow field inside tube are very complicated.

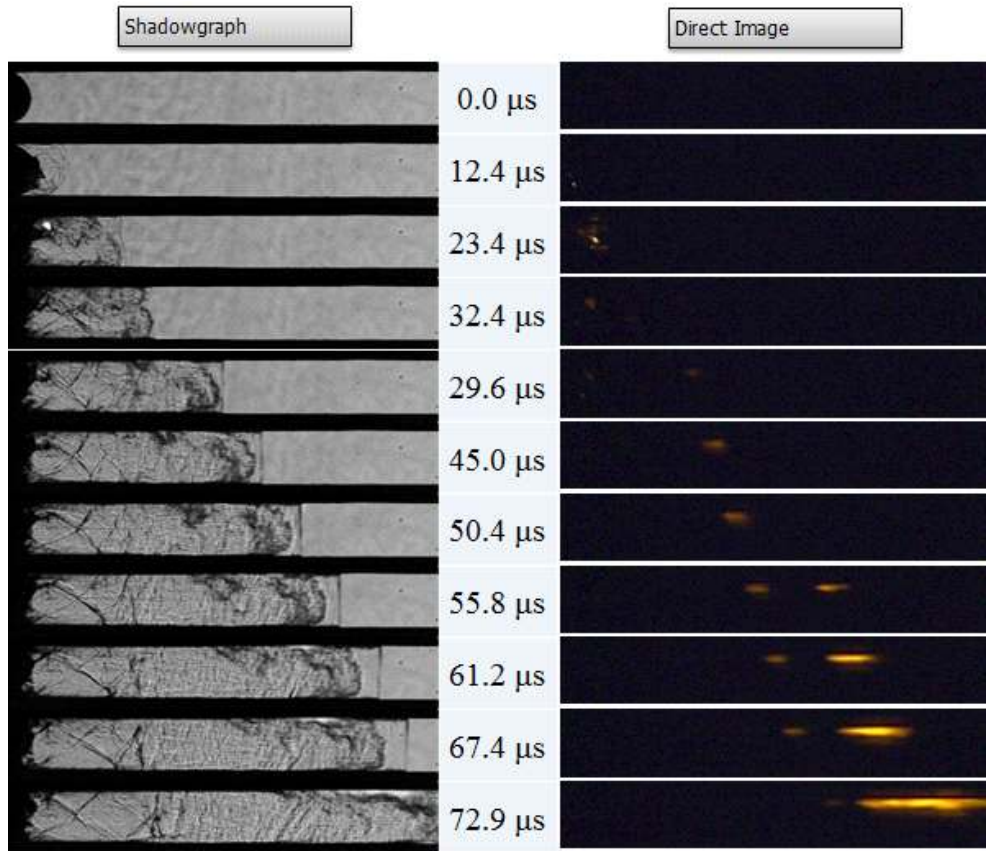


Figure 13 Representative test result (Test #90)

Just after diaphragm rupture, flow distortion from the side edge of the burst hole creates accelerated mixing between air and released hydrogen at contact surface. Besides, shock induced by diaphragm rupture reflect from tube wall, and reflected shocks concentrate in the core area of the tube and making high pressure area at flow core. This reflected shock induced high pressure area effect to leading shock changing shape. After that, mixing between hot air heated by shock and cold hydrogen accelerated. And finally ignited from near tube walls where the mixing process is most developed.

But in this experimental study, we could not observe the vortex ring that

was shown in former numerical study. It is expected that this vortex ring phenomena takes very short time to be captured in high speed camera or too small density variation to be captured in shadowgraph images.

In direct image, it is observed that small flamelet are occurring just after diaphragm rupture. Generally, it is taking place in flow core area. This early flamelet occurs in 20 μ s after the diaphragm rupture. Flamelet stand for 30 μ s and extinguished. This is expected that core high pressure, temperature area then former mentioned. When the diaphragm ruptures, diaphragm ruptures in a hemispherical shape. Leading shock is formed from rupture as also hemispherical shape. When rupture pressure is going over critical pressure then core high pressure temperature areas are satisfied hydrogen auto ignition environment. and in mixing area between hot air heated by shock and cold hydrogen, the flame was ignited. this reaction area extinguished soon because leaked high pressure hydrogen pushes air, and isolate flame from oxidizer.

main reaction area of self-ignition phenomena take place downstream from wall boundary layer. the main reaction region tendency are similar to previous studies.

From this results, initial diaphragm rupture shapes are effect to intial flamelet but not effect to entire self-ignition. also we can discover that shock direct ignition that happen in early flame area could not stand on ignition and mainly effective reaction area take place later where hydrogen and hot air mixing is very active. so if shock strength enough to make air hot to hydrogen auto ignition, then molecular mixing is governing the self-ignition phenomena.

4.2 Test results

Test conditions shown in Table 4. in accordance with diaphragm has different rupture pressure, some times thinner diaphragm test burst higher pressure than thicker diaphragm.

Experimental results are compared with theoretically calculated values are followed Table 5.

Table 5 Summary of test; theoretical shock speed.

test #	test gas	rupture pressure (MPa)	shock speed theoretical (m/s)	shock speed measured (m/s)	error (%)
#77	Helium	4.1	1065	934	12
#81	Hydrogen	4.3	1237	1212	2
#89	Hydrogen	8.6	1515	1441	4
#90	Hydrogen	8.6	1515	1519	<1
#91	Hydrogen	9.2	1545	1514	2
#92	Hydrogen	9.4	1553	1440	7

Shock strength is measured by tube pressure transducer from pressure jump when shock moving through pressure transducer. Shock speed also measured from distance between pressure transducers and measured pressure jump time.

Self-ignition were observed over 8.0 MPa just like previous studies.

In this study, the main goal is observing how leading shock occur and develop and how leading shock shapes influences to entire self-ignition phenomena. Shadowgraph and high speed direct images are applied to observing shock waves and flowfield in the extension tube. Also for validating test condition measuring shock strength and shock speed, 6 pressure transducers were applied to lower part of extension tube.

figure. 14 shows typical flow configuration in the extension tube after diaphragm rupture and leading shock fully developed. Between leading shock and mixing front, there were complex shock interactions. It was verified as oblique shocks originated from tube wall discontinuity gap by sensor port hole. This is similar as previous study[4-5, 12].

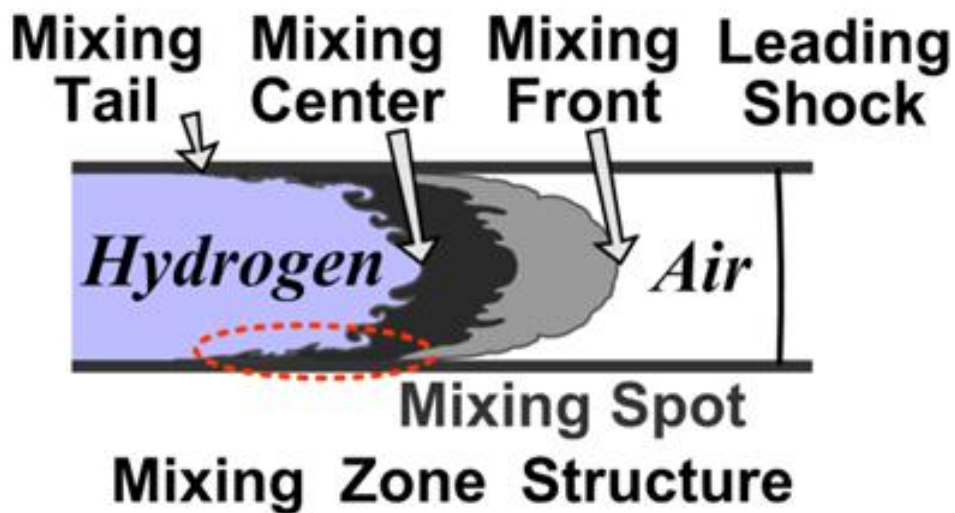


Figure 14 Leading shock wave and mixing zone model schematic [12]

4.2.1 Low pressure test

For identifying differences between test gases, low pressure test are conducted. Hydrogen and helium were used for test gas pressure. Test number 77 and 81 are conducted with 100 μ m thick film as diaphragm. but 77 test used helium and 81 used hydrogen.

From figure 15 and figure 17, because of difference of molecular weight of hydrogen and helium, there were little differences between each tests on shock speed and shock strength. This differences can be expected from shock tube theory.

Also, Figure 15 shows that measured pressures are slightly lower than theoretical value. It is expected that the measured rupture storage pressure is not only measure static pressure but also measure dynamic pressure from gas feeding speed. So rupture storage pressure and theoretical values are slightly over measured. Differences between measured pressure and theoretical value were under 5%.

Measured pressure from P1 always lower than other and theoretical value. it is expected as leading shock pass P1 before fully developed.

Shadowgraph result shows that there were no considerable differences between hydrogen test and helium test.

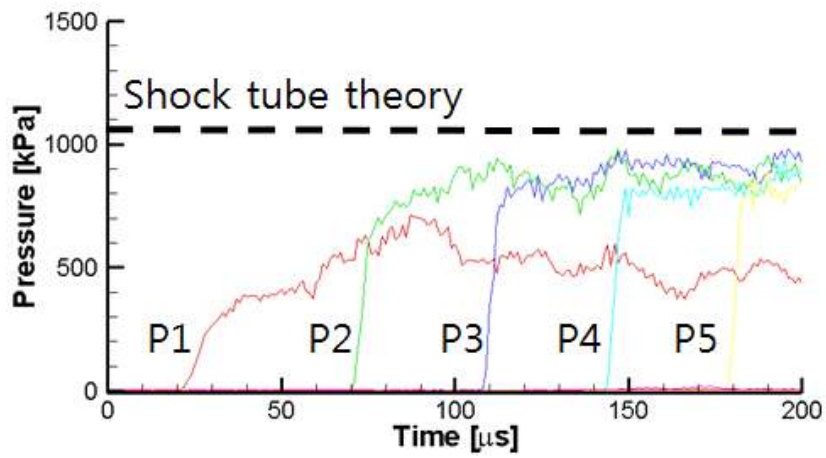


Figure 15 Wall static pressure of extension tube; Test #77

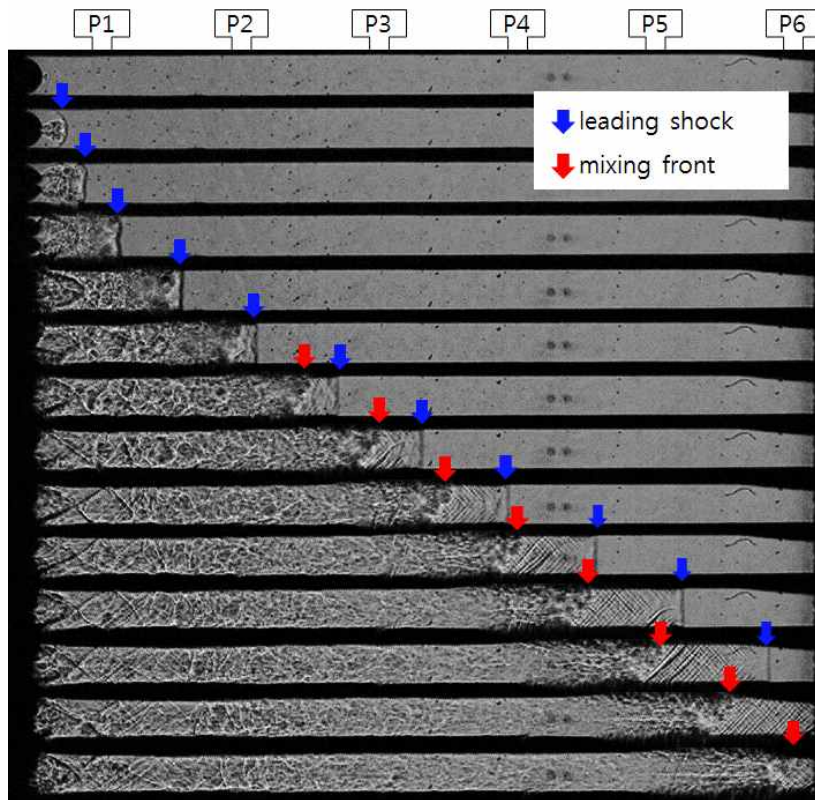


Figure 16 Shadowgraph image, entire area, non-ignition; Test #77

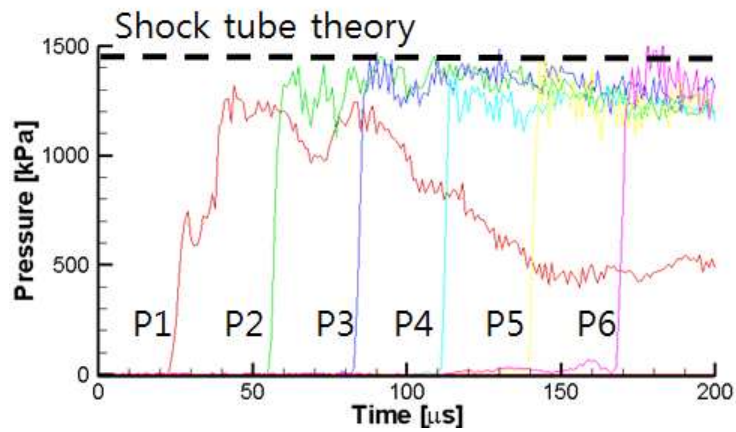


Figure 17 Wall static pressure of extension tube; Test #81

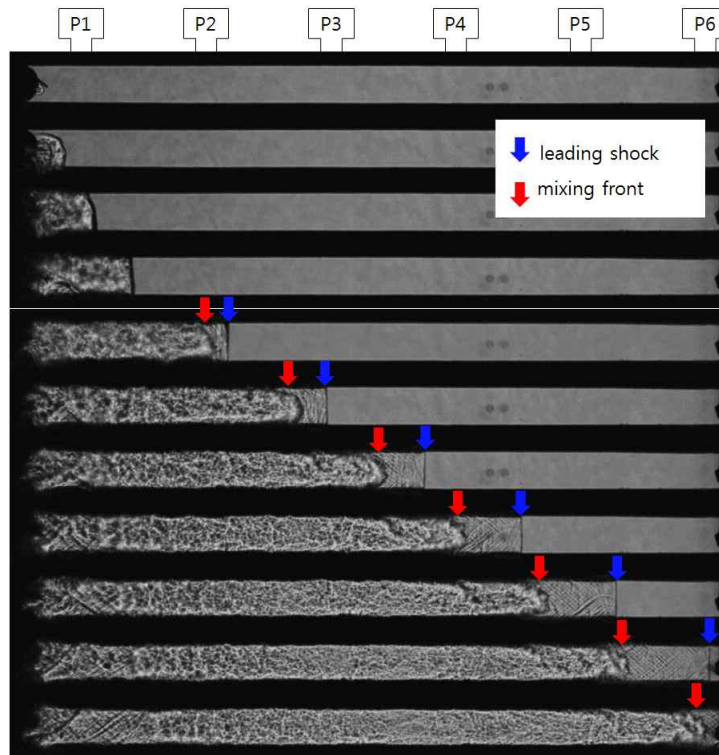


Figure 18 Shadowgraph image, entire area, non-ignition; Test #81

4.2.2 High pressure test

To identifying how diaphragm rupture condition affects to high pressure hydrogen self-ignition, high pressure test were conducted. Diaphragm films used for high pressure test has 200 μm and 219 μm thickness. Storage pressures when diaphragm ruptured are about 8.5 MPa for 200 μm film and about 9.0 MPa for 219 μm .

The result of measuring the pressure shows that measured pressure are fine matched with shock tube theoretical values. because rupture pressure goes higher, effect of dynamic pressure by test gas feeding flow are goes smaller.

The results of shadowgraphs and direct images are as followed. every high pressure test has self-ignitions. test #89 and #90 has same diaphragm film thickness and similar rupture pressure.

Test #89 has strong early flame area. This early flame area takes place with about 20 μs after rupture, hold out 30 μs and extinguished. This flame is expected with following mechanism. Leading shock heats air once and reflects on tube wall. The reflected shock heated air again and interaction with leading shock and other reflected shock. This complex shock interactions enhances hydrogen-air mixing. Heated hydrogen-air mixture makes auto-ignition. But following hydrogen flow pushes air into downstream, isolates flame from air makes blow off. the Second flame ignited from mixing zone boundary layer about 50 mm downstream of diaphragm at about 50 μs after diaphragm rupture. This flame developed to core flow for exit of extension tube and stand for out of extension tube. From this result, we varied that mainly effective flame for hydrogen self-ignition is second ignited flame from mixing zone boundary layer. Also, governmental phenomenon is hydrogen-air mixing then shock direct ignition.

Test #90 goes similar with test #89. But in this case, ruptured film debris ignited in early flame area. Flamelet from early flame runs into downstream. this flames are also blown out in about 30 μ s. Main flame which affects to self-ignition, ignited 50 mm downstream of diaphragm at about 50 μ s after diaphragm rupture. Compared with test #89 and #90, it looks as early flames did not affect to entire hydrogen self-ignition phenomenon. Mainly effective flames are ignited in similar place and time regardless with early flame strength.

In test #91, diaphragm ruptures in upper side. and has early flame area. Early flame looks weaker than test #89. It is expected Early flames are not only affect burst pressure but also effected from flow field and shock structure. In this case, faster hydrogen flow makes early flame ignite harder. Test #92 shows this effect more clearly. In this case, rupture pressure is higher then #91 or #89, but it looks there were no early flames.

Test #91 and #92, main flame ignited in about 65 mm downstream form diaphragm, at about 50 μ s after diaphragm ruptures in both cases.

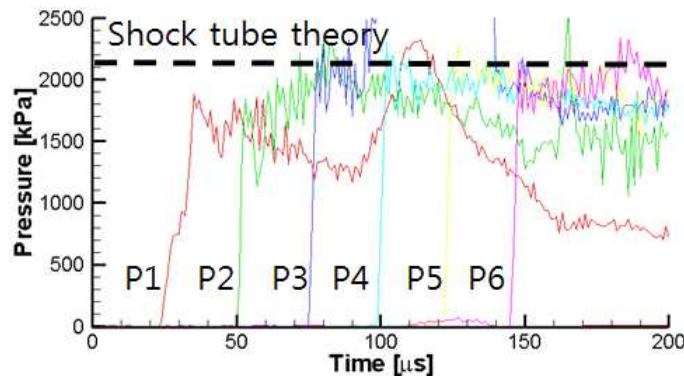


Figure 19 Wall static pressure of extension tube;
Test #89

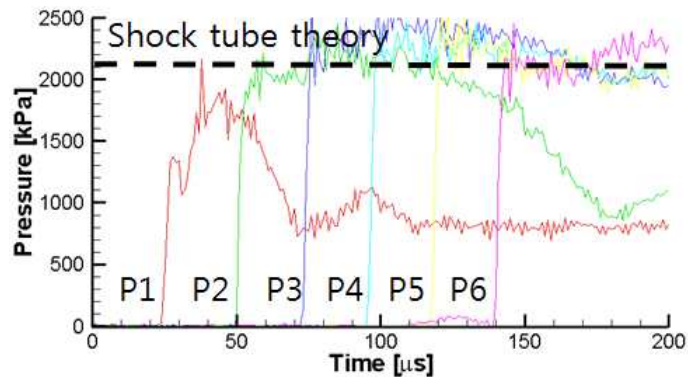


Figure 20 Wall static pressure of extension tube;
Test #90

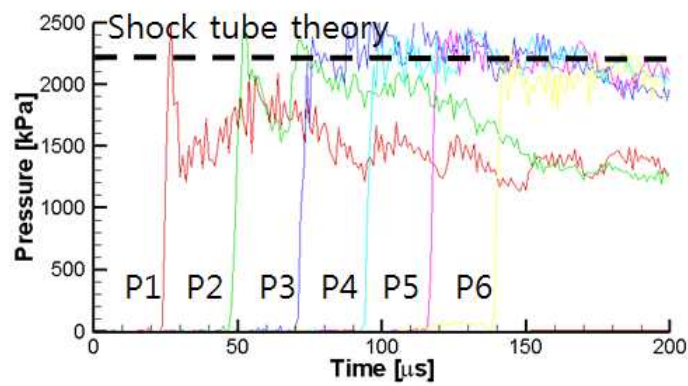


Figure 21 Wall static pressure of extension tube;
Test #91

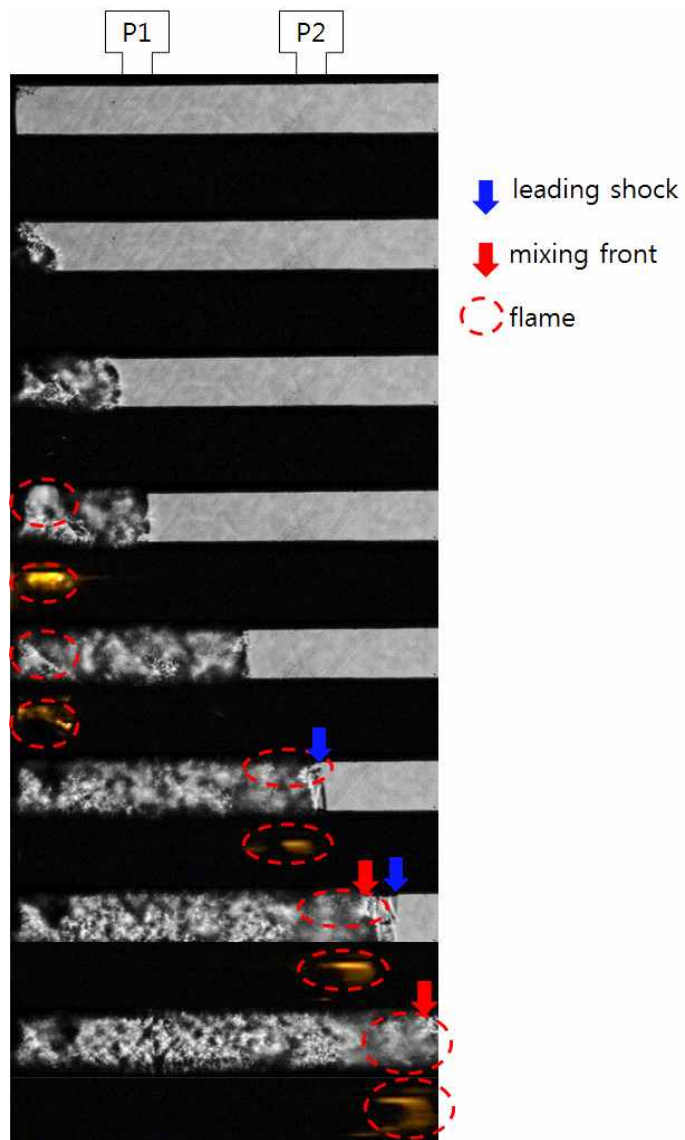


Figure 22 Upstream area visualization of test #89

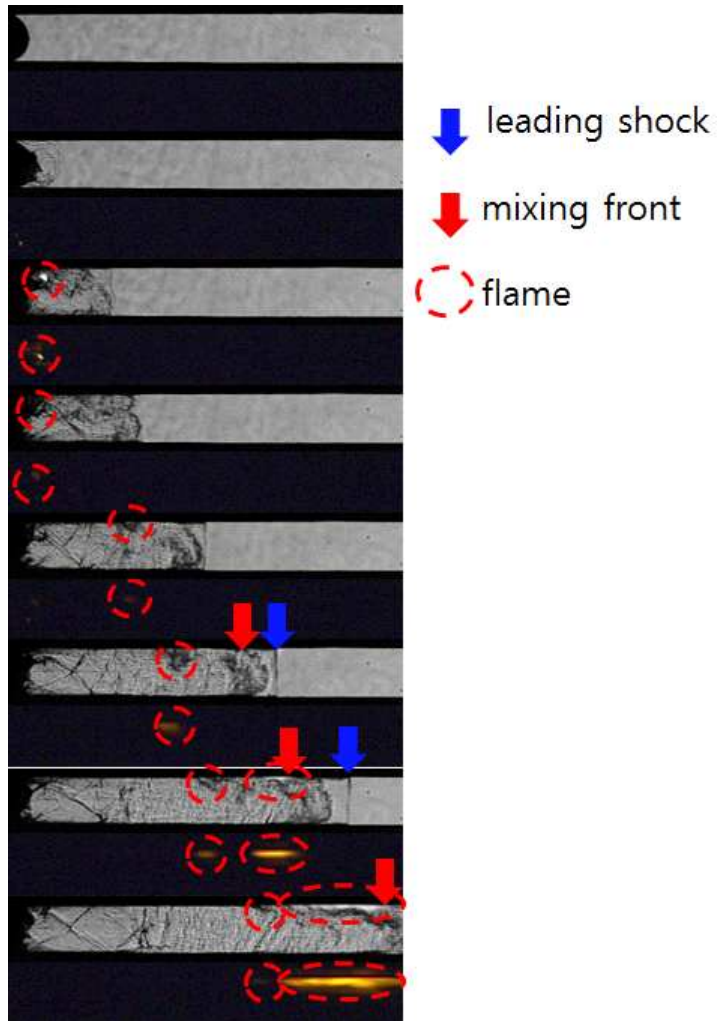


Figure 23 Upstream area visualization of test #90

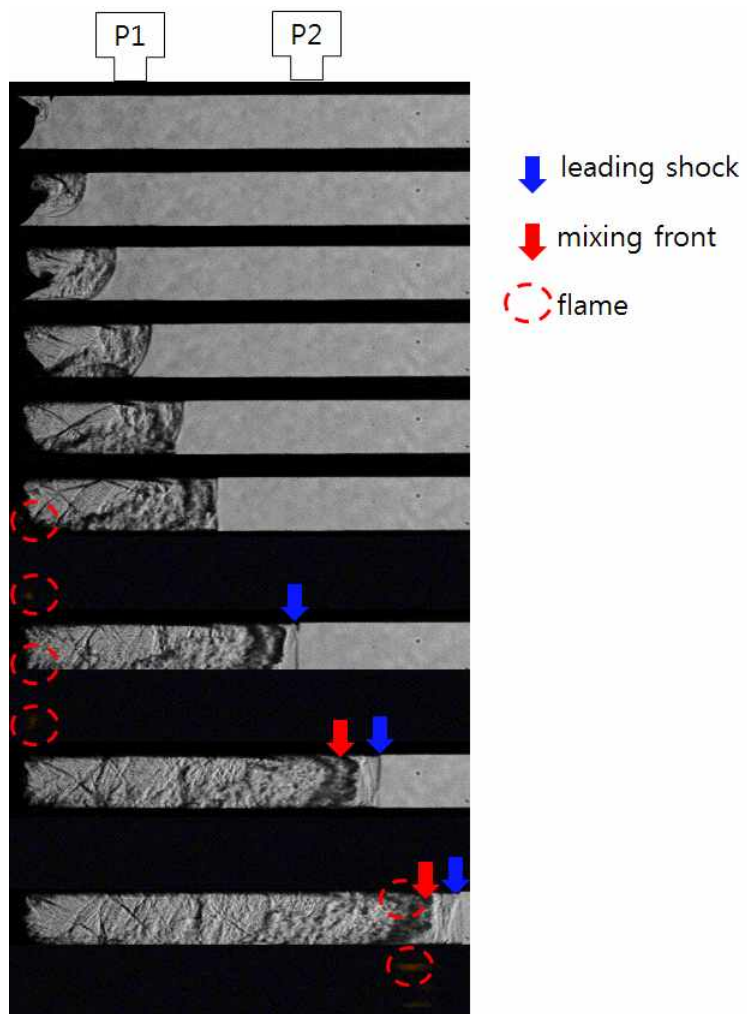


Figure 24 Upstream area visualization of test #91

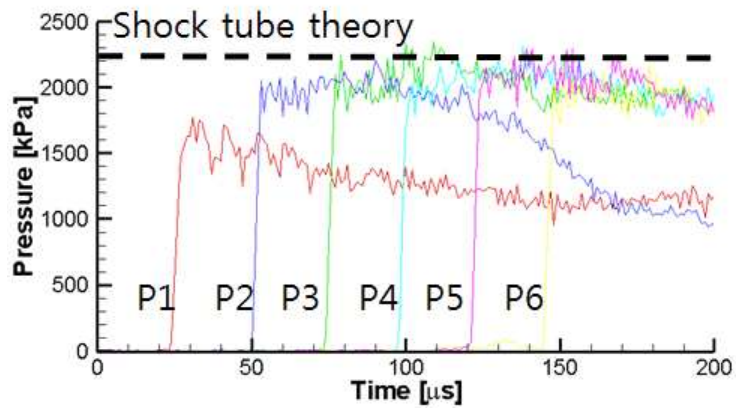


Figure 25 Wall static pressure of extension tube; Test #92

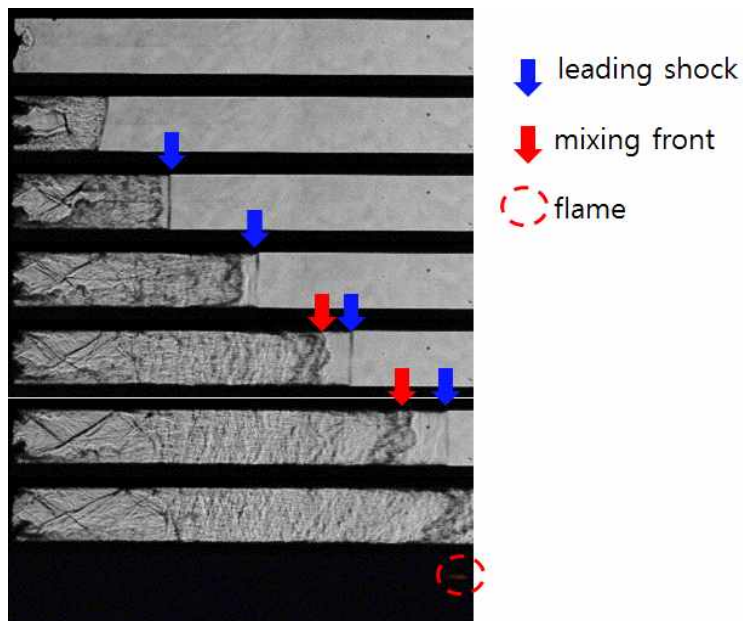


Figure 26 Upstream area visualization of test #92

Chapter 5. Conclusion

In this study, self-ignition phenomena was studied when high pressure hydrogen suddenly released into extension tube with shadowgraph and high-speed direct photography, and pressure measurements. shape of shock, flow field, and reaction field are observed. Main focus is how diaphragm rupture shape effect to self-ignition phenomena.

Leading shocks shapes are very different from each other according diaphragm rupture shapes and position. It is observed that how leading shock can be distorted, hemispheric leading shock transform to flat planer shock while shock travels to tube exit. Mainly effective reaction areas for hydrogen self-ignition are in boundary layer mixing zone following leading shock. Mixing zone is formed just after diaphragm rupture. no matter diaphragms where the rupture the mixing zone form similary regardless with diaphragm rupture shape.

Another found is early flame. It takes place very after diaphragm rupture. it take place $20\mu s$ after diaphragm bursts and it stands for $30\mu s$. It seems like early flames are affected by not only rupture pressure but also flow field and shock structure. But, test results shows that main effective flame of high pressure hydrogen self-ignition ignited at downstream mixing zone boundary layer. This shows that the governmental phenomenon is hydrogen-air mixing rather than shock direct ignition.

In conclusion, diaphragm rupture condition like rupture shape or rupture position, effect to flow field or shock structure inner extension tube that make effect to early flames. But consequentially, it has no direct effect on entire self-ignition process of high pressure hydrogen suddenly released into tube

Bibliography

- [1] G.R. Astbury, S.J. Hawksworth, “Spontaneous Ignition of Hydrogen Leaks: A Review of Postulated Mechanisms”, *Int. J. Hydrogen Energy* 32 (21)(2007) 2178-2185.
- [2] P. Wolanski, S. Wojcicki, “Investigation into the Mechanics of the Diffusion Ignition of a Combustible Gas Flowing into an Oxidizing Atmosphere”, *Proc. Combust. Inst.* 14(1972) 1217-1223.
- [3] F.L. Dryer, M. Chaos, Z. Zhao, J.N. Stein, J.Y. Alpert, C.J. Homer, “Spontaneous Ignition of Pressurized Releases of Hydrogen and Natural Gas into Air”, *Combust. Sci. Technol.* 179(4)(2007) 663-694.
- [4] T. Mogi, D. Kim, H. Shiina, S. Horiguchi, “Self-ignition and Explosion during Discharge of High-pressure Hydrogen”, *J. Loss Prevent. Proc. Indus.* 21(2)(2008) 199-204
- [5] T. Mogi, Y. Wada, Y. Ogata, A. K. Hayashi, “Self-ignition and Flame Propagation of High-pressure Hydrogen Jet during Sudden Discharge from a Pipe”, *Int. J. Hydrogen Energy* 34(2009) 5810-5816.
- [6] V.V. Golub, D.I. Baklanov, T.V. Bazhenova, M.V. Bragin, S.V. Golovastov, M.F. Ivanov, “Shock-induced Ignition of Hydrogen Gas during Accidental or Technical Opening of High-pressure Tanks”, *J. Loss Prevent. Proc. Indus.* 20(2007), 439-446
- [7] V.V. Golub, D.I. Baklanov, S.V. Golovastov, M.E. Ivanov, I.N. Laskin, A.S. Saveliev, N.V. Semin, V.V. Volodin, “Mechanisms of High-pressure Hydrogen Gas Self-ignition in Tubes”, *J. Loss Prevent. Proc. Indus.* 21 (2)(2008) 185-198
- [8] V.V. Golub, D.I. Baklanov, T.V. Bazhenova, S.V. Golovastov, M.F. Ivanov, I.N. Laskin, N.V. Semin, V.V. Volodin, “Experimental and

Numerical Investigation of Hydrogen Gas Auto-ignition”, Int. J. Hydrogen Energy 34(2009) 5946-5953

[9] H.J. Lee, Y.R. Kim, S.H. Kim, I.S. Jeung, “Experimental Investigation on the Self-ignition of Pressurized Hydrogen Released by the Failure of a Rupture Disk Through Tubes”, Proc. Combust. Inst. 33(2011) 2351-2358

[10] B.J. Lee, I.S. Jeung, “Numerical Study of Spontaneous Ignition of Pressurized Hydrogen Released by the Failure of a Rupture Disk into a Tube”, Int. J. Hydrogen Energy, 34(21)(2009) 8763-8769

[11] J.X. Wen, B.P. Xu, V.H.Y. Tam, “Numerical Study on Spontaneous Ignition of Pressurized Hydrogen Release Through a Length of Tube”, Combust. Flame 156(11)(2009) 2173-2189

[12] Y.R. Kim, “A Flow Visualization Study on Self-ignition of High Pressure Hydrogen Gas Released into a Tube” (PhD diss., Seoul National University, 2013)

초 록

높은 연소 효율로서 수소는 이상적인 미래의 차세대 에너지원으로 주목받고 있다. 현재로서는 수소를 저장함에 있어 고압으로 압축하여 고압 용기에 저장하는 방법이 가장 현실성 있는 저장 방법으로 알려져 있다.

그러나 이러한 고압 저장 방법은 용기가 파손 되었을 때 심각한 위협을 초래할 수 있는 잠재성을 가지고 있다. 또한 고압의 수소 용기가 파열하였을 때, 원인이 불명확한 수소의 자발 점화 현상이 관측되어 왔다.

고압의 수소가 공기 중으로 방출되었을 때 발생하는 수소의 자발 점화 현상의 원인 메커니즘을 이해하는 것은 수소를 실용화 하는데 있어서 매우 중요하다. 이러한 수소의 자발 점화 메커니즘을 규명하기 위해서 많은 수치 해석적, 실험적 연구가 수행 되었다. 이전의 연구를 통하여 격막 파열 직후의 복잡한 유동과 충격과 구조가 수소 자발 점화의 원인으로 알려졌었다. 격막의 파열 형상에 따른 전체 고압 수소 자발 점화 현상에 끼치는 영향은 중요하다. 그럼에도 이전 연구에서는 연구 모델의 한계로 격막 파열 직후 격막의 파열 형상이 전체 수소 자발 점화 과정에 끼치는 영향을 실험적으로 확인하는데에 한계가 있었다. 이 논문에서는 누출 튜브에 설치된 가시화 창을 격막 부근 까지 연장하였다. 초고속 카메라를 적용한 쉘도우 그래프 기법과 직접광 촬영을 통하여 격막 주변의 파열 직후의 유동을 가시화 하여 수소의 자발 점화 메커니즘을 더욱 명확히 하고자 하였다. 유동 가시화 결과를 보안하기 위해 별도의 압력 측정도 수행되었다. 다양한 격막 파열 형상에서 수소의 자발 점화 과정을 관측 하였다. 실험 결과 이러한 격막 파열 형상은 초기에 복잡한 유동장과 충격과 구조를 형성하여 초기 화염 영역을 형성 하는데 영향을 끼쳤다. 그러나 이렇게 발생한 초기 화염 영역은 금방 소화되며, 전체 수소 자발 점화에 주요한 영향을 끼치는 화염은 초기의 복잡한 유동장과 충격과 구조, 초기 화염 유무와 관계없이 같은 파열 압력에서 일정한 거리와 시간을 두고 점화 되었다. 이러한 결과에서 격막의 파열 형상이 수소의

자발 점화 현상에 끼치는 영향은 미미하며, 수소와 공기의 혼합이 충격 파에 의한 유동의 가열보다 수소의 자발 점화 현상에 더 주요한 지배 현상이라는 결론을 얻을 수 있었다.

주요어 : 고압 수소, 자발 점화, 유동 가시화, 수소-공기 혼합

학 번 : 2013-20708